Journal of Sol-Gel Science and Technology 26, 721–725, 2003

Sol-Gel Routes to Zeolite Membranes and Thin Films

S. KALLUS
CNRS, Institut Européen des Membranes, 1919 Route de Mende, 34293 Montpellier, France

A. HAHN
Institut for Inorg. Chem., Johannes Gütenberg Univ. Mainz, Germany

G. GOLEMME
Dip. di Ingegneria Chimica e dei Materiali, Univ. Calabria, Rende, Italy

C. ALGIERI
Instituto di Ricerca su Membrane e Modellistia di Reattori Chimici-CNR, Rende, Italy

P. TIMMINS
Institut Laue Langevin, 38042 Grenoble, France

J.D.F. RAMSAY*
CNRS, Institut Européen des Membranes, 1919 Route de Mende, 34293 Montpellier, France
ramsay@crit.univ-montp2.fr

Abstract. The synthesis of zeolite membranes and thin films using the secondary growth process is briefly described. In this process colloidal zeolite particles (sols) are prepared hydrothermally and then subsequently deposited on substrates to produce uniform layers of controlled thickness, as illustrated with silicalite and zeolite-A. The formation and growth of the zeolite sols has been investigated in situ by small angle neutron scattering (SANS). SANS measurements on silicalite sols at progressively higher concentrations have provided details of the colloid interactions which lead to zeolite gel-layer structures which are uniform and free of defects.

Keywords: colloidal zeolites, film formation, zeolite membranes, small-angle neutron scattering

Introduction

Zeolites are crystalline alumino-silicate or silicate materials which have a highly regular and open microporous (<2 nm) structure [1]. Almost a hundred different structural types of zeolite are known. Each of these has a distinct pore size, shape and interconnectivity. Because of these properties, zeolites can interact very selectively with adsorbed molecules. These exceptional properties have lead to numerous technical applications for zeolites in bulk powder form (heterogeneous catalysis, gas separation, adsorption). However more recently there has been a surge of interest in the potential applications of thin films or membranes of zeolites. These include highly selective separation membranes [2, 3], sensors, conductors, and optoelectronic devices [4]. In such applications thin layers of material are required which must be highly uniform and free of defects.

*To whom all correspondence should be addressed.

Several methods for the fabrication of zeolite thin films have recently been reported [3]. A common route used to produce membranes for gas separation involves zeolite crystallization onto a substrate (e.g. a porous ceramic) under in situ hydrothermal conditions. This method is generally satisfactory, although it has been difficult to control the membrane thickness and uniformity. In an attempt to overcome this problem, "secondary growth" methods are now being developed [2, 5]. These involve two-stages. Firstly, zeolite is produced in a colloidal form by a hydrothermal reaction in the precursor solution. The colloidal zeolite particles are then separated and deposited on a substrate as a thin uniform layer. In a second stage this thin layer is then subjected to a further hydrothermal treatment. In this process the colloidal particles act as seeds for secondary growth, thus producing a uniform membrane layer. In order to optimise the secondary growth route a better understanding of the first stage of the method is required. This includes (a) the process of zeolite colloid formation, and (b) the mechanism by which the colloidal particles are consolidated to give a continuous layer structure. An insight into both of these aspects has been achieved using small angle neutron scattering (SANS) as described here. The SANS technique is particularly appropriate because it can be used for in situ measurements even under hydrothermal conditions, and also when the colloidal particle concentration is very high. Work on two different zeolite systems—silicalite (MFI) and zeolite A (LTA) will be illustrated here.

Experimental

Zeolite A colloids with an approximate size of 300 nm were produced from a prehydrolysed solution containing silicate and aluminate oligomers with the composition $1SiO_2$:$0.59Al_2O$:2.6TMAOH:0.25NaOH:$100H_2O$. The precursor solution was heated at 353 K for 72 hours. Colloidal zeolite was extracted from the milky solution by centrifugation. The product was redispersed in water and centrifugations repeated until the pH of the colloidal dispersion was 10.3.

Silicalite-1 colloids were prepared using routes similar to that described previously by Schoeman and co workers [6, 7]. For the SANS investigations, the composition of the precursor solution was: $1SiO_2$:4EtOH:0.36TPAOH:0.01NaOH:$19H_2O$. The kinetics

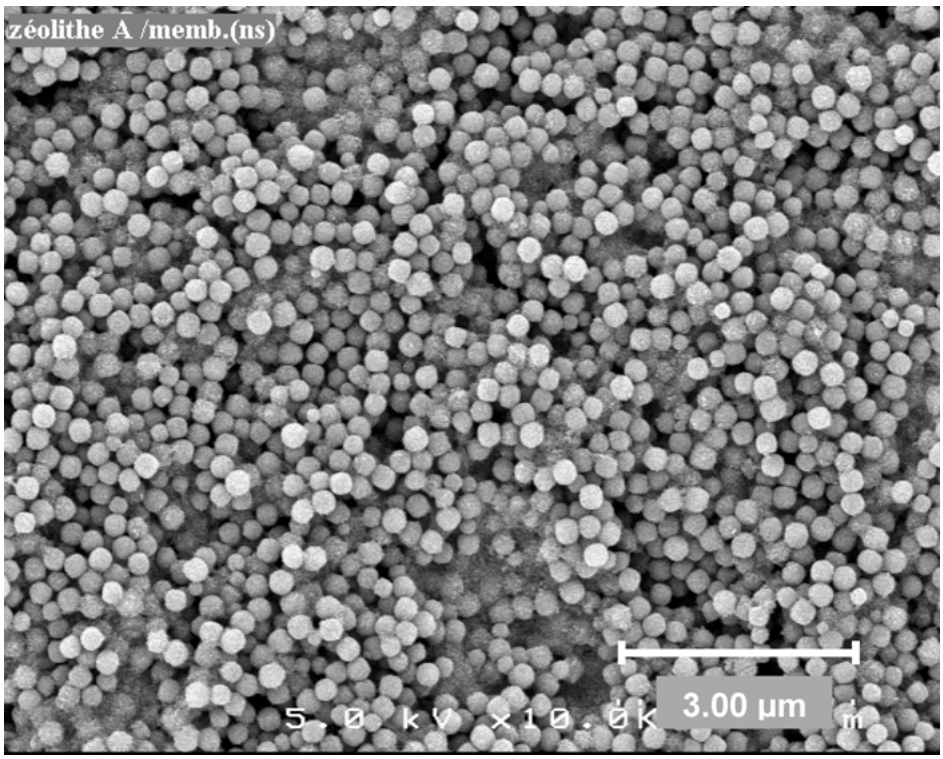

Figure 1. SEM of colloidal zeolite A particles.

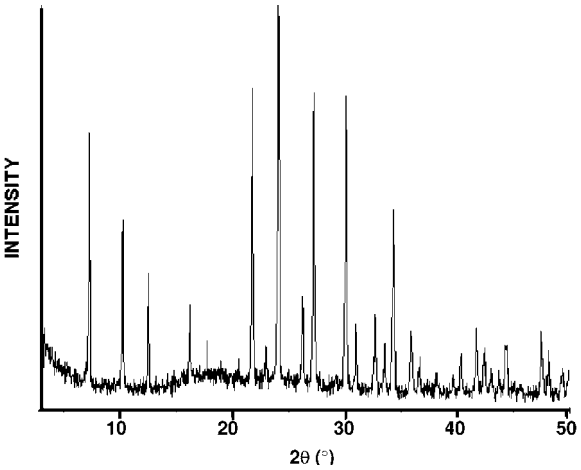

Figure 2. X-ray diffraction pattern of zeolite A particles showing LTA structure.

of colloid formation at 363 K were followed by SANS measurements on this reaction solution at intervals over a period of approximately 22 hours. Other SANS measurements were made on a series of samples having a progressively increasing particle concentration, which eventually resulted in a solid phase. The size of the colloidal particles in this series corresponded to that after approximately 20 hours reaction time. SANS measurements were made at the Institut Laue Langevin, Grenoble, using the small angle scattering instrument, D22, as described previously [8]. Measurements were made in a momentum transfer range, Q, of 2×10^{-3} to $>2.5 \times 10^{-2}$ Å^{-1}, where $Q = 4\pi \sin\theta/\lambda$, and λ is the neutron wavelength. Zeolite samples were characterized by SEM and XRD as previously [9].

Results and Discussion

Zeolite LTA

The SEM of a dried sample of washed zeolite-A showed spherical colloidal particles with a diameter of ~320 nm (Fig. 1). X-ray diffraction (Fig. 2) confirmed that this material had the crystalline LTA structure although it was associated with an amorphous component as evident from the significant broad background.

When a colloidal dispersion in water was dried on a substrate a uniform layer of particles was formed as illustrated in Fig. 3. Here the substrate is an anodic alumina membrane disc (Anopore™ , Whatman, UK)

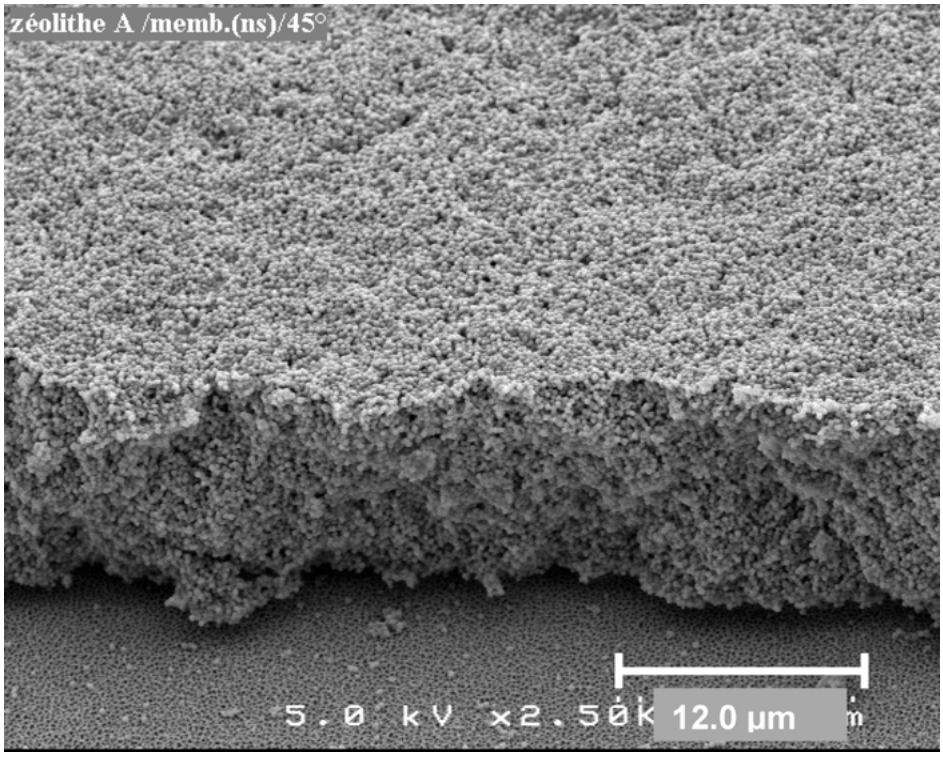

Figure 3. SEM of layer of zeolite A particles deposited on an Anopore® alumina membrane support.

with a nominal pore size of 20 nm. It will be noted that the zeolite layer has a uniform thickness of $\sim$10 μm and that the packing of the colloidal particles is efficient and regular. This latter feature will be explored in more detail with the silicalite system.

Silicalite-1

The evolution of the SANS during hydrothermal treatment of the silicalite-1 precursor solution is illustrated in Fig. 4. This shows that the scattered intensity, $I(Q)$, is hardly significant during an induction period of nearly 18 hours. Thereafter, $I(Q)$ increases rapidly, corresponding to the formation and accelerating growth of colloid particles. After 20 hours the SANS corresponds to colloid particles with a diameter of $\sim$80 nm, which are quite uniform in size. SEM results also confirmed that the particles were approximately spherical and of similar size after 20 hours. At higher resolution the particles had a "cauliflower-like" appearance and seemed to be formed by clusters of much smaller subunits. The XRD (Fig. 5) confirms the silicalite-1 struc.

SANS measurements were also made on a series of samples of increasing colloid concentrations to obtain an insight into the mechanism by which the particles give rise to a consolidated layer structure. Results in Fig. 6 are for particles formed after approximately 20 hours reaction. At the lowest volume fraction, ϕ, of 2%, the form of the scattering is similar to that in Fig. 4, corresponding to non-interacting particles with a diameter of $\sim$80 nm. However as the concentration is increased there is evidence of interference in the SANS. This is evident in the pronounced maximum

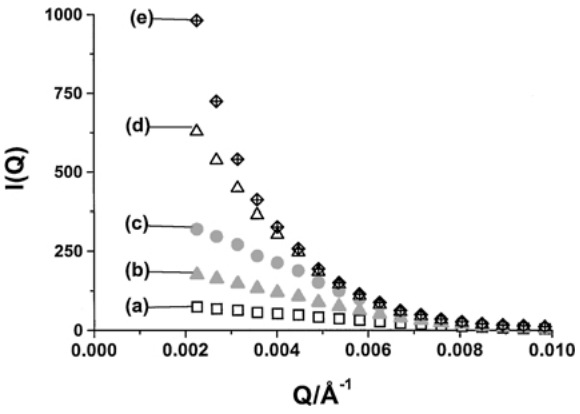

Figure 4. Kinetic evolution of SANS during the hydrothermal (363 K) synthesis of colloidal silicalite-1. After, (a) 18 h, (b) 19 h, (c) 20 h, (d) 21 h, (e) 22 h.

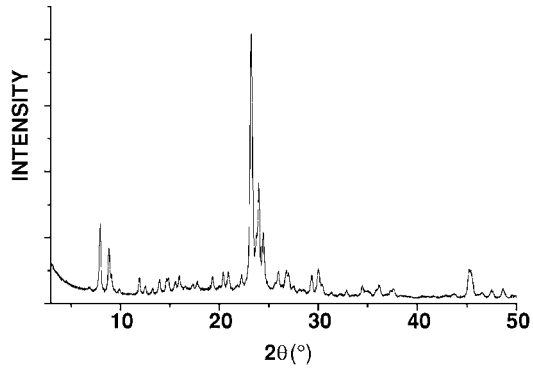

Figure 5. X-ray diffraction pattern of colloidal silicalite-1.

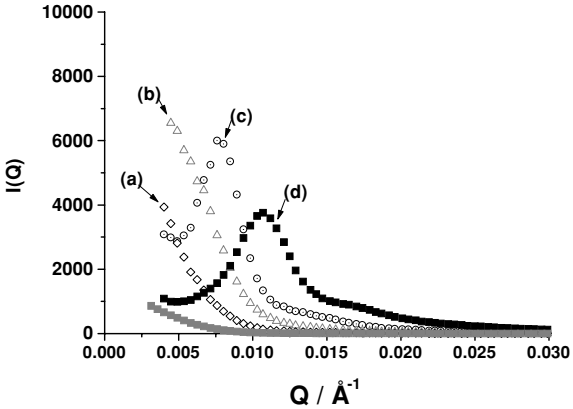

Figure 6. SANS of colloidal zeolite particle dispersions showing effects of increasing volume fraction (diameter of particles is approximately 80 nm). Particle volume fractions, Φ, are: (a) 0.02, (b) 0.05, (c) 0.15, (d) dried solid.

which occurs at $Q \sim 8 \times 10^{-3}$ Å^{-1} for the dispersion with $\phi = 15\%$. This feature can be ascribed to an ordering of the particles due to inter-particle repulsion forces. Such effects have already been described in detail for sol-gel particle systems, such as silica, ceria [10] and clay particle dispersions [11] for example. The position of this maxima corresponds to an approximate inter-particle spacing of 0.08 μm. For the solid phase the position of the interference peak is shifted to a higher Q of 0.010 Å^{-1}, indicating a closer particle separation of approximately 0.063 μm. This separation is slightly smaller than the apparent particle diameter, which tentatively suggests some inter-penetration or coalescence between the colloid particles. A more confident interpretation of the structure in the zeolite layer will be obtained from further detailed analysis of SANS and electron microscopy investigations. However it is already evident that a solid layer is formed

by zeolite particles having a high packing density and short-range order. Such a compact structure may be important in the subsequent secondary growth process employed to produce defect-free zeolite membranes.

References

1. R.M. Barrer, *Zeolites and Clay Minerals as Sorbents and Molecular Sieves* (Academic Press, New York, 1978).
2. M. Tsapatis and G.R. Gavalas, in *MRS Bulletin 24: Membranes and Membrane Processes,* edited by V.N. Burganos (Mat. Res. Soc., New York, 1999), p. 30.
3. J.D.F. Ramsay and S. Kallus, in *Recent Advances in Gas Separation by Microporous Membranes,* edited by N.K. Kanellopoulos (Elsevier, Amsterdam, 2000), p. 373.
4. G. Cho, J.S. Lee, D.T. Glatzhofer, B.M. Funf, W.L. Yan, and E.A. O'Rear, Adv. Mater. **11**, 497 (1999).
5. C. Algieri, G. Golemme, S. Kallus, and J.D.F. Ramsay, Micropor. and Mesopor. Mater., in press.
6. A.E. Person, B.J. Schoeman, J. Sterte, and J.E. Otterstedt, Zeolites **14**, 557 (1994).
7. J. Hedlund, S. Mintova, and J. Sterte, Micropor. Mesopor. Mater. **28**, 185 (1999).
8. *ILL Yellow Book*, Guide to Neutron Research Facilities at ILL (ILL, Grenoble, 2001).
9. S. Kallus, P. Langlois, G.E. Romanos, Th. Steriotis, E.S. Kikkinides, N.K. Kanellopoulos, and J.D.F. Ramsay, in *Studies in Surface Science and Catalysis,* edited by K.K. Unger, G. Kreysa and J.P. Baselt (Elsevier, Amsterdam, 2000), p. 467.
10. J.D.F. Ramsay, Chem. Soc. Rev. **15**, 335 (1986).
11. J.D.F. Ramsay and P. Lindner, J. Chem. Soc. Faraday Trans. **89**, 4207 (1993).